Mechanical Systems and Signal Processing (2001) **15**(2), 323–336
doi:10.1006/mssp.2000.1331, available online at http://www.idealibrary.com on IDEAL®

STIFFNESS NON-LINEARITY CLASSIFICATION THROUGH STRUCTURED RESPONSE COMPONENT ANALYSIS USING VOLTERRA SERIES

ANIMESH CHATTERJEE AND N. S. VYAS

Department of Mechanical Engineering, Indian Institute of Technology, Kanpur, India.
E-mail: vyas@iitk.ac.in

(Received 13 December 1999, and in final form 10 August 2000)

Most non-linear analysis problems, consider only the Duffing oscillator as a representative case. In engineering analysis, it is however, also important to recognise the type of non-linearity actually influencing the system. A procedure, involving structured higher-order FRF analysis based on Volterra theory is suggested in the present work, to distinguish a polynomial form of non-linearity from other possible forms. Volterra theory provides concepts of linear, bilinear, trilinear, etc. kernels, which upon convolution with the excitation force and subsequent summation can be employed to represent the response of a non-linear system. The kernels of the system are understood as multidimensional unit impulse response functions. The Volterra series response representation is employed in this work to facilitate its processing in a structured manner, to extract characteristic features, which can help in placing the system non-linearity in an appropriate class. The Volterra series platform is also employed to make a distinction between symmetric and asymmetric forms of the restoring force function. A multi-tone excitation procedure is further suggested, through which higher-order kernels of the system can be constructed for identification of the structure of the polynomial representing the restoring force. The procedures are illustrated through numerical simulation.

1. INTRODUCTION

Characterisation of dynamic systems, from input–output data, is broadly categorised into parametric and non-parametric identifications. Parametric identification refers to systems where sufficient *a priori* information about the mathematical structure of the class to which the system belongs, is available. The identification procedure in such cases is reduced to an estimation of system parameters through a search in parameter space. Non-parametric identification concerns modelling in a function space by input–output mapping, for systems where sufficient information on the mathematical structure or class is not available.

While identification procedures for linear systems are fairly well establilshed [1, 2], the wide variety of non-linearities exhibited by physical systems, makes the non-linear system identification problem complex. A review of identification procedures, in applications involving networks and devices, has been done by Haber and Unbehauen [3] for various classes of non-linearity, such as Weiner model, Hammerstein model, Weiner–Hammerstein model. Boyd *et al.* [4] and Chua and Liao [5, 6] have discussed higher-order kernel identification procedures based on Volterra series. Masri and Caughy [7] and Masri *et al.* [8] have suggested non-parametric methods for mechanical spring–mass systems based on restoring force mapping technique. Works in the area of parametric identifications generally assumes the polynomial structure or a specific non-polynomial structure, and then the procedure for parameter estimation is suggested. Rice and Fitzpatrick [9] have estimated quadratic damping due to drag force using random excitation and spectral density approach. Mottershed and Stanway [10] have developed procedure for estimation on nth power non-linear damping. Bendat and Peirsol [11] estimated quadratic stiffness of wave forces in terms of a stochastically equivalent polynomial form. Studies have been carried out by Tiwary and Vyas [12], and Khan and Vyas [13] for rotor-bearing systems modelled as Duffing oscillator.

However, the parametric procedures suffer from the inherent assumption of the form of non-linearity. The prediction of the future behaviour of the identified system may be in substantial error unless the mathematical model represents the essential characteristics of the physical system. Research works in the area of system structure identification, particularly for the mechanical systems, are very few. Nayfeh [14] has suggested a combination of perturbation and free vibration test for identification of certain non-linear characteristics such as hysteresis, different forms of damping, presence of self-oscillatory terms, etc. Bendat *et al.* [15] developed a general identification technique from measured input–output stochastic data for a wide range of non-linearities such as Duffing oscillator, Van-der Pol oscillator, dead band and clearance non-linearity.

In the present work, an identification procedure based on Volterra series is suggested for classification between polynomial and non-polynomial form of non-linearities. Further, by using the properties of higher-order kernel transforms, the series structure of the polynomial form is also identified. The procedure has been outlined for a polynomial up to the cubic term and it can be extended for structures containing higher-order terms.

2. VOLTERRA SERIES RESPONSE REPRESENTATION

For a single-degree-of-freedom system

$$m\ddot{x}(t) + c\dot{x}(t) + g[x(t)] = f(t) \tag{1}$$

where $g[x(t)]$ and $f(t)$ represent the non-linear restoring force and applied excitation respectively. The response can be expressed, in a functional series form, using Volterra series as

$$x(t) = x_1(t) + x_2(t) + x_3(t) + \cdots \tag{2}$$

with $x_n(t)$ as the nth-order response component given by

$$x_n(t) = \int_{-\infty}^{\infty} \cdots \int_{-\infty}^{\infty} h_n(\tau_1, \ldots, \tau_n) f(t-\tau_1) \cdots f(t-\tau_n)\, \mathrm{d}\tau_1 \cdots \mathrm{d}\tau_n \tag{3}$$

$h_n(\tau_1, \ldots, \tau_n)$ is the nth-order Volterra kernel. The nth-order frequency response function, obtained through Fourier transform of the nth-order Volterra kernel, is

$$H_n(\omega_1, \omega_2, \ldots, \omega_n) = \int_{-\infty}^{\infty} \int_{-\infty}^{\infty} \cdots \int_{-\infty}^{\infty} h_n(\tau_1, \tau_2, \ldots, \tau_n) \prod_{i=1}^{n} \mathrm{e}^{-j\omega_i \tau_i}\, \mathrm{d}\tau_1\, \mathrm{d}\tau_2, \ldots, \mathrm{d}\tau_n. \tag{4}$$

For single-tone harmonic excitation

$$f(t) = A\cos\omega t = \frac{A}{2}\mathrm{e}^{j\omega t} + \frac{A}{2}\mathrm{e}^{-j\omega t} \tag{5}$$

the response components of equation (2) are obtained as

$$x_1(t)=\frac{A}{2}H_1(\omega)\mathrm{e}^{j\omega t}+\frac{A}{2}H_1(-\omega)\mathrm{e}^{-j\omega t}$$

$$x_2(t)=\frac{A^2}{2}H_2(\omega,-\omega)+\frac{A^2}{4}H_2(\omega,\omega)\mathrm{e}^{j2\omega t}+\frac{A^2}{4}H_2(-\omega,-\omega)\mathrm{e}^{-j2\omega t}$$

$$x_3(t)=\frac{A^3}{8}H_3(\omega,\omega,\omega)\mathrm{e}^{j3\omega t}+\frac{3A^3}{8}H_3(\omega,\omega,-\omega)\mathrm{e}^{j\omega t}+\frac{3A^3}{8}H_3(\omega,-\omega,-\omega)\mathrm{e}^{-j\omega t}$$

$$+\frac{\mathrm{A}^3}{8}H_3(-\omega,-\omega,-\omega)\mathrm{e}^{-j3\omega t}. \tag{6}$$

The general expression for the nth-order response component becomes

$$x_n(t)=\left(\frac{A}{2}\right)^n\sum_{p+q=n}{}^nC_qH_n^{p,q}(\omega)\mathrm{e}^{j\omega_{p,q}t} \tag{7}$$

where the following brief notations have been used:

$$H_n^{p,q}(\omega)=H_n(\underbrace{\omega,\omega,\dots,}_{p\text{ times}}\ \underbrace{-\omega,-\omega,\dots}_{q\text{ times}})\quad\text{and}\quad\omega_{p,q}=(p-q)\omega.$$

The total response of the system can then, be expressed as

$$x(t)=\sum_{n=1}^{\infty}\left(\frac{A}{2}\right)^n\sum_{p+q=n}{}^nC_qH_n^{p,q}(\omega)\mathrm{e}^{j\omega_{p,q}t}. \tag{8}$$

It is evident from the structure of various response components [equation (6)], that odd harmonics appear only in odd-order response components and even harmonics appear only in even-order response components. An odd-order response component $x_{2m+1}(t)$ comprises of odd harmonics $\omega, 3\omega, \dots, (2m+1)\omega$, while an even-order response component $x_{2m}(t)$ contains a constant d.c. term and even harmonics $2\omega, 4\omega, \dots, 2m\omega$. This structured form of Volterra series response components can form the basis for classification of non-linearity between polynomial and non-polynomial forms. The first few response components can be separated [16, 17] through excitation of the system at different force levels, $\alpha, \beta, \gamma, \dots$ and measurement of the resultant responses $x_{(\alpha)}(t), x_{(\beta)}(t), x_{(\gamma)}(t)\dots$ to get

$$\begin{bmatrix}x_{(\alpha)}(t)\\x_{(\beta)}(t)\\x_{(\gamma)}(t)\end{bmatrix}=\begin{bmatrix}\alpha&\alpha^2&\alpha^3\\\beta&\beta^2&\beta^3\\\gamma&\gamma^2&\gamma^3\end{bmatrix}\begin{bmatrix}x_1(t)\\x_2(t)\\x_3(t)\end{bmatrix}+\begin{bmatrix}e_1\\e_2\\e_3\end{bmatrix}. \tag{9}$$

e_i are the truncation errors which are generally neglected while solving equation (9) for extracting the response components. The frequency contents of the separated response components $x_1(t), x_2(t), x_{(3)}(t)\dots$ can be employed to indicate whether the system is having a polynomial form of non-linearity or not.

3. IDENTIFICATION OF POLYNOMIAL NON-LINEARITY FORM

A frequency domain analysis of the various component orders is carried out to distinguish a polynomial form of the non-linear restoring force $g[x(t)]$, in the governing equation

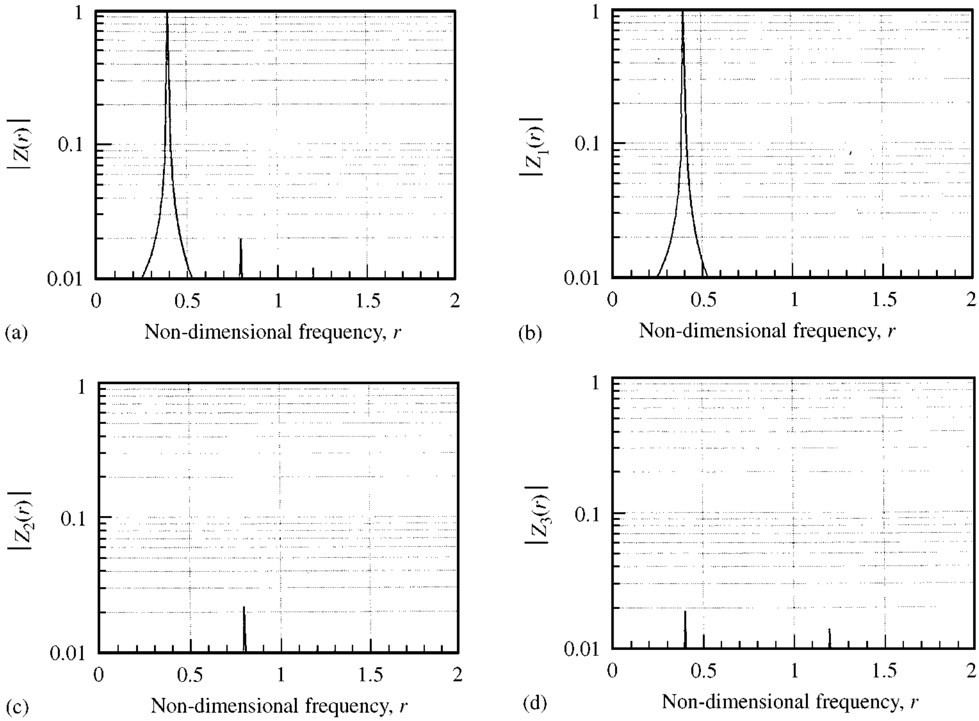

Figure 1. Response component spectra for $g[x(t)] = k_1 x(t) + k_2 x^2(t) + k_3 x^3(t)$: (a) total response; (b) first-order response component; (c) second-order response component; (d) third-order response component.

(1), from non-polynomial forms (e.g. bilinear, coulomb, pth power type, etc.). Figure 1(a) typically shows the response spectrum of a system with a general polynomial form of non-linearity

$$g[x(t)] = k_1 x(t) + k_2 x^2(t) + k_3 x^3(t). \tag{10}$$

The non-dimensional response $z(\tau) = x(t)/(A/k_1)$ has been numerically simulated through a fourth-order Runge–Kutta algorithm, for a set of non-dimensional parameters: $r = \omega/\sqrt{k_1/m} = 0.4$; $\varsigma = c/2\sqrt{k_1 m} = 0.01$; $\lambda_2 = k_2 A/k_1^2 = 0.01$; $\lambda_3 = k_3 A^2/k_1^3 = 0.015$, where the non-dimensional time $\tau = \sqrt{k_1/m}\,t$. The response components, $z_1(\tau)$, $z_2(\tau)$, $z_3(\tau)$ are separated using the order component separation technique of equation (9). Figures 1(b), (c) and (d), respectively show the Fourier transforms $\hat{z}_1(r)$, $\hat{z}_2(\mathrm{r})$ and $\hat{z}_3(r)$ of the components. It can be seen that the first response component spectrum $\hat{z}_1(r)$ contains only the first harmonic at $r = 0.4$, second response component spectrum $\hat{z}_2(r)$ contains the second harmonic at $2 \times r = 0.8$ alone, while the third response component spectrum $\hat{z}_3(r)$ contains the first and third harmonics. This observation is in confirmation with the structure of the order components as given in equation (6). However, a non-polynomial form of non-linearity does not exhibit such ordered harmonic characteristics. Figure 2(a) gives the Fourier transform of the simulated response for a system with non-linearity given by

$$g[x(t)] = kx(t)|x(t)|. \tag{11}$$

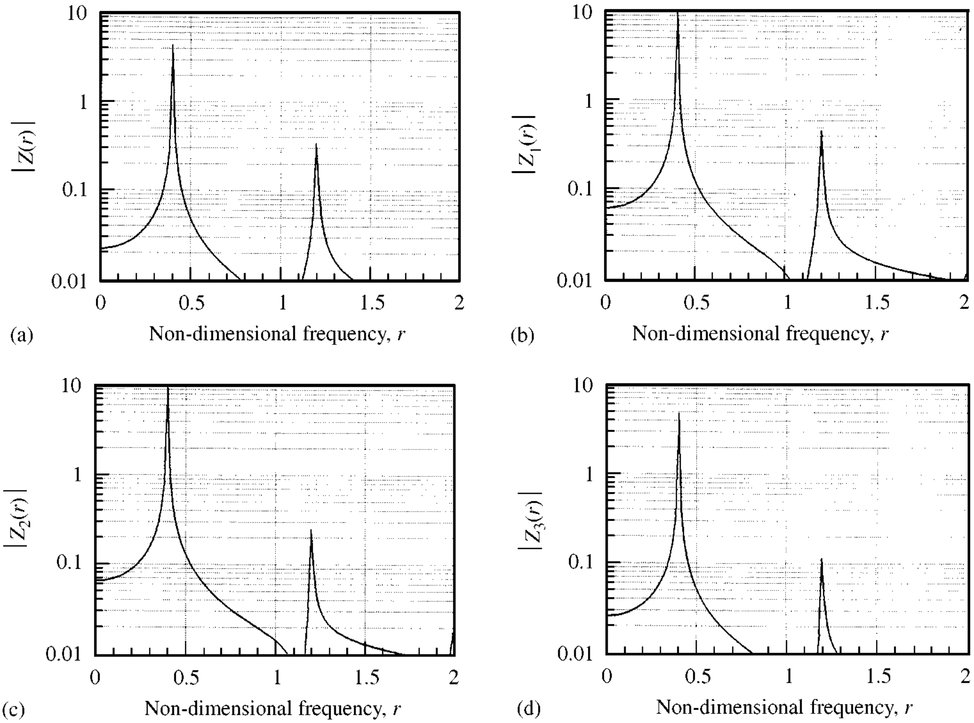

Figure 2. Response component spectra for $g[x(t)] = kx(t)|x(t)|$: (a) total response; (b) first-order response component; (c) second-order response component; (d) third-order response component.

It is to be noted that a non-linearity of above type can be expressed as a polynomial, with constant coefficients only for a constant range of response amplitude. The coefficients of the polynomial approximations, in general, are functions of response amplitudes. The Fourier transforms [Figs 2(a)–(d)] of the response components, in this case do not show the kind of structured behaviour, as seen in the case of polynomial non-linearity [Figs 1(b)–(d)]. Similar disorder is observed in the case of a bilinear form of non-linear function, given by

$$g[x(t)] = kx(t) \tag{12}$$

with the dual stiffness values $k = c_1$ for $x(t) > 0$ and $k = c_2$ for $x(t) < 0$. The Fourier transforms of the non-dimensional response $z(\tau)$ and the first response component $z_1(\tau)$ are shown in Figs 3(a) and (b), for $c_1 = 0.9$, $c_2 = 1.0$ and non-dimensional frequency equal to 0.4. However, the second- and third-order components, $z_2(\tau)$ and $z_3(\tau)$ are found to be zero. Other commonly occurring non-polynomial form of non-linearity, where the damping and stiffness forces take the form $a[x^2(t) - 1]\dot{x}(t)$ (Van-der Pol oscillator); $c\dot{x}(t) + kx(t) \pm F_d$ (Coulomb damper); $\beta\dot{x}(t)|\dot{x}(t)| + kx(t)$ (quadratic damping); $c\dot{x}(t) + kx^p(t)\mathrm{sgn}(x)$ (for a fractional power p, as in rolling element bearings) also do not exhibit an ordered form, as discussed earlier, when their response is treated as a Volterra series comprising of various ordered components. These observations can be explained by the fact that, the procedure for ordered component separation remains valid only if the system kernels are amplitude independent. For a polynomial form of non-linearity, the system kernels

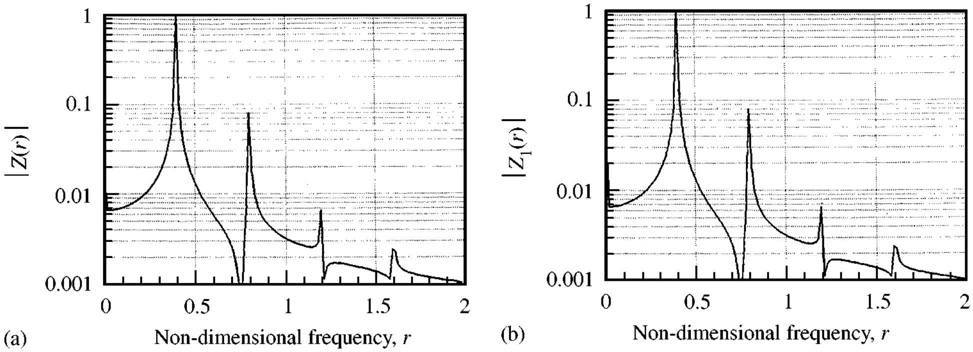

Figure 3. Response component spectra for $g[x(t)] = kx(t)$; $k = 0.9$, for $x(t) > 0$, $k = 1.0$, for $x(t) < 0$: (a) total response; (b) first-order response component.

are independent of response amplitude and function of system parameters only. This is seen by substitution of the Volterra series response expression (8), in the equation of motion (1), which yields

$$H_1(\omega) = 1/(-m\omega^2 + k + jc\omega) \quad \text{for } n = 1 \tag{13a}$$

$$H_n^{p,q}(\omega) = -\frac{H_1(\omega_{p,q})}{{}^nC_q} \times \left[\begin{array}{l} k_2 \sum\limits_{\substack{p_i+q_i=n_i \\ n_1+n_2=n}} \{{}^{n_1}C_{q_1} H_{n_1}^{p_1,q_1}(\omega)\} * \{{}^{n_2}C_{q_2} H_{n_2}^{p_2,q_2}(\omega)\} + \\ k_3 \sum\limits_{\substack{p_i+q_i=n_i \\ n_1+n_2+n_3=n}} \{{}^{n_1}C_{q_1} H_{n_1}^{p_1,q_1}(\omega)\} * \{{}^{n_2}C_{q_2} H_{n_2}^{p_2,q_2}(\omega)\} * \{{}^{n_3}C_{q_3} H_{n_3}^{p_3,q_3}(\omega)\} \end{array} \right] \quad \text{for } n > 1. \tag{13b}$$

While, the first-order kernel transform [equation 13(a)] is a function of the system's linear parameters alone, in addition to the excitation frequency, the higher-order kernel transforms $H_n^{p,q}(\omega)$ are functions of lower-order kernel transforms and non-linear parameters [equation 13(b)]. For non-polynomial non-linearity, such expression of kernels in amplitude-independent form is not possible. An equivalent polynomial form, in such cases, gives rise to amplitude-dependent system parameters through its coefficients. This results in amplitude-dependent kernel transforms. Subsequently, the application of the method of ordered component separation, which involves variation of the excitation amplitude, gives inconsistent results.

These observations constitute the identification procedure for polynomial form of non-linearity, whereby a given system can be subjected to a sinusoidal excitation and the Volterra series response components $x_1(t)$, $x_2(t)$, $x_3(t)$ are extracted through equation (9). Compliance of the Fourier transforms of these response components with the harmonic component structure of equation (6) can be checked. The system can be classified as having a polynomial form of non-linearity in its restoring force if an odd-order response component, $x_{2m+1}(t)$, contains only odd harmonics ω, 3ω, ... ,$(2m + 1)\omega$, while an even-order response component $x_{2m}(t)$, if present, comprises of even harmonics 2ω, 4ω, ... , $2m\omega$ alone. If the spectra of the response components do not exhibit above ordered characteristics, the system non-linearity cannot be classified as polynomial form.

4. DISTINCTION BETWEEN SYMMETRIC AND ASYMMETRIC POLYNOMIAL FORMS

A polynomial form of non-linearity, can be further identified as symmetric or asymmetric, through analysis of the even and odd harmonic of the response components. For a symmetric non-linearity (e.g. as in Duffing oscillator), where

$$g[x(t)] = -g[-x(t)] \tag{14}$$

only odd orders $x_{2m+1}(t)$ of the response $x(t)$ exist. The even orders $x_{2m}(t)$ are zero. Expressing a symmetric form polynomial non-linearity of the restoring force in a system through

$$m\ddot{x}(t) + c\dot{x}(t) + k_1 x(t) + k_3 x^3(t) + k_5 x^5(t) + \cdots = f(t) \tag{15}$$

and multiplying the above equation by -1, one gets

$$-m\ddot{x}(t) - c\dot{x}(t) - k_1 x(t) - k_3 x^3(t) - k_5 x^5(t) - \cdots = -f(t).$$

Noting that, $-x^{2m+1}(t) = [-x(t)]^{2m+1}$, the above equation can be rewritten as

$$m[-\ddot{x}(t)] + c[-\dot{x}(t)] + k_1[-x(t)] + k_3[(-x(t))^3] + k_5[(-x(t))^5] + \cdots = -f(t). \tag{16}$$

If $\bar{x}(t)$ be the response for a negative excitation, $-f(t)$, so that the governing equation is

$$m\ddot{\bar{x}}(t) + c\dot{\bar{x}}(t) + k_1\bar{x}(t) + k_3\bar{x}^3(t) + k_5\bar{x}^5(t) + \cdots = -f(t) \tag{17}$$

comparison of equations (15) and (16) gives

$$x(t) + \bar{x}(t) = 0 \tag{18}$$

i.e. for a symmetric non-linear system, the sum of response under excitations $f(t)$ and $-f(t)$ become zero. However, a system with asymmetric non-linearity with at least an even power term $k_{2m}x^{2m}(t)$ in its governing equation, provides $[-x(t)]^{2m} = [x(t)]^{2m}$, leading to $x(t) + \bar{x}(t) \neq 0$.

Since Volterra series is a power series, multiplying excitation by negative sign will result in multiplying the response component $x_n(t)$ by $(-1)^n$, which gives

$$\bar{x}(t) = -x_1(t) + x_2(t) - x_3(t) + \cdots. \tag{19}$$

Addition of the above equation with equation (2), which gives the response for an excitation $f(t)$ and further application of condition in equation (17) for a symmetric polynomial non-linearity gives

$$x_2(t) + x_4(t) + \cdots = 0. \tag{20}$$

As the above equation is to be satisfied for all excitation levels, it implies that

$$x_2(t) = 0, \quad x_4(t) = 0, \ldots .$$

Now, since even-order harmonic of the excitation frequency ω appear only in even-order response components $x_2(t), x_4(t), \ldots$ [equation (6)], the above leads to the conclusion that the response $x(t)$, of a system with symmetric polynomial non-linearity will be devoid of any even order harmonics of the excitation frequency (Fig. 4). However, even harmonics will appear in response of asymmetric non-linear systems (Fig. 5).

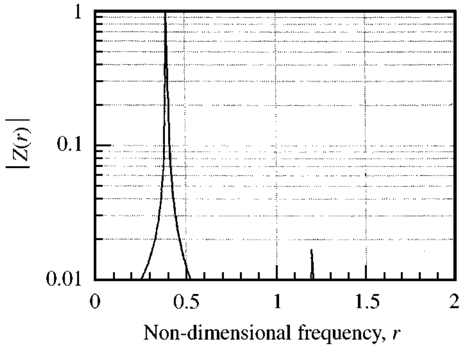

Figure 4. Response spectrum for $g[x(t)] = k_1 x(t) + k_3 x^3(t)$.

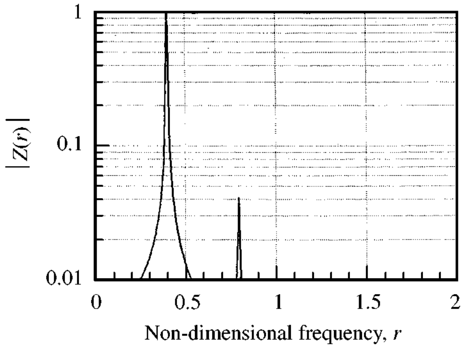

Figure 5. Response spectrum for $g[x(t)] = k_1 x(t) + k_2 x^2(t)$.

5. IDENTIFICATION OF THE POLYNOMIAL SERIES STRUCTURE

Identification of the structure of polynomial series representing the non-linear stiffness function $g[x(t)]$ is carried out through probing of higher-order Volterra kernel transforms of the system, which are obtained through subjecting the system to multi-tone excitation forces. Such multi-harmonic signals can be readily simulated on a computer. An electrodynamic shaker, connected to the computer through an analogue to-digital card and an amplifier can be employed to provide excitation to the system. The present analysis is restricted to a third degree polynomial, i.e.

$$g[x(t)] = k_1 x(t) + k_2 x^2(t) + k_3 x^3(t). \tag{21}$$

Identification is made between the following cases:

(i) $k_2 = 0$ and $k_1, k_3 \neq 0$.
(ii) $k_3 = 0$ and $k_1, k_2 \neq 0$.
(iii) $k_1, k_2, k_3 \neq 0$.

Considering a three-tone excitation $f(t) = A\cos\omega_1 t + B\cos\omega_2 t + C\cos\omega_3 t$ in equation (1), with $g[x(t)] = k_1 x(t) + k_2 x^2(t) + k_3 x^3(t)$, the Volterra series response components, $x_n(t)$, can be written as

$$x_n(t) = \frac{1}{2^n} \sum_{\substack{p+q+s+u \\ +v+w=n}} A^{p+q} B^{s+u} C^{v+w}\, C_{p,q,s,u,v,w} H_n^{p,q,s,u,v,w} e^{j\omega_{p,q,s,u,v,w}} \tag{22}$$

where

$$C_{p,q,s,u,v,w} = \frac{n!}{p!\, q!\, s!\, u!\, v!\, w!} \qquad \omega_{p,q,s,u,v,w} = (p-q)\omega_1 + (s-u)\omega_2 + (v-w)\omega_3$$

and

$$H_n^{p,q,s,u,v,w} = H_n(\underbrace{\omega_1, \ldots,}_{p \text{ times}} \underbrace{-\omega_1, \ldots,}_{q \text{ times}} \underbrace{\omega_2, \ldots,}_{s \text{ times}} \underbrace{-\omega_2, \ldots,}_{u \text{ times}} \underbrace{\omega_3, \ldots,}_{v \text{ times}} \underbrace{-\omega_3, \ldots,}_{w \text{ times}}).$$

The Volterra kernel transforms, $H_1(\omega_1)$, $H_2(\omega_1, \omega_2)$ and $H_3(\omega_1, \omega_2, \omega_3)$, can be obtained from the component response harmonic amplitudes, $X_1(\omega_1)$, $X_2(\omega_1 + \omega_2)$ and $X_3(\omega_1 + \omega_2 + \omega_3)$, using equation (22), as

$$H_1(\omega_1) = X_1(\omega_1)/A \tag{23a}$$

$$H_2(\omega_1, \omega_2) = X_2(\omega_1 + \omega_2)/AB \tag{23b}$$

$$H_3(\omega_1, \omega_2, \omega_3) = \frac{X_3(\omega_1 + \omega_2 + \omega_3)}{(3ABC/4)}. \tag{23c}$$

Figures 6 and 7 show the second- and third-order kernel transforms $H_2(\omega_1, \omega_2)$ and $H_3(\omega_1, \omega_2, \omega_3)$ obtained from the numerically simulated response to the three-tone excitation for the three cases of polynomial structures mentioned above. (These kernel transforms have been plotted for a range of ω_1/ω_n and ω_2/ω_n, keeping ω_3/ω_n fixed at a value of 0.6). It is rather simple to distinguish the first case ($k_2 = 0$ and $k_1, k_3 \neq 0$) from the other two by noting that the second-order Volterra kernel $H_2(\omega_1, \omega_2)$ is identically equal to zero, over the entire frequency range in this case, as seen from the following synthesised expressions of higher-order kernel transforms [using equation (13)]:

$$H_2(\omega_1, \omega_2) = -k_2 H_1(\omega_1) H_1(\omega_2) H_1(\omega_1 + \omega_2) \tag{24}$$

$$H_3(\omega_1, \omega_2, \omega_3) = H_1(\omega_1) H_1(\omega_2) H_1(\omega_3) H_1(\omega_1 + \omega_2 + \omega_3) \times \left[\frac{2}{3} k_2^2 \{ H_1(\omega_1 + \omega_2) + H_1(\omega_2 + \omega_3) + H_1(\omega_1 + \omega_3) \} - k_3 \right]. \tag{25}$$

Equations (24) and (25) above can also be referred to similarly recognise second-order combination peaks at $\omega_1 + \omega_2 = \omega_n$, $\omega_2 + \omega_3 = \omega_n$ and $\omega_2 + \omega_3 = \omega_n$, in the third-order kernel transform map of $H_3(\omega_1, \omega_2, \omega_3)$ for cases (ii) and (iii). These combination peaks can be seen to be absent in case (i). This characteristic feature distinguishes the symmetric case (i) from cases (ii) and (iii), which are asymmetric.

Distinction can be made between the asymmetric cases (ii) and (iii) by further investigating the third-order kernel transform, $H_3(\omega_1, \omega_2, \omega_3)$. Figures 8(a) and (b) show the third-order kernel transform $H_3(\omega_1, \omega_2, \omega_n)$, with $\omega_3 = \omega_n$, for cases (ii) and (iii), respectively. Both plots show peaks at frequency combinations (a) $\omega_1 = \omega_n$, $\omega_2 = \omega_n$; (b) $\omega_1 = \omega_n$, $\omega_2 = 0$; (c) $\omega_1 = 0$, $\omega_2 = \omega_n$ [peaks (b) and (c) are identical due to reasons of symmetry].

Distinction can be made between cases (ii) and (iii) by a comparison between the peaks of (b) [or (c)] with that occurring at the frequency combination (a). Using equation (25), the ratio of these peak values becomes

$$\frac{H_3(0, \omega_n, \omega_n)}{H_3(\omega_n, \omega_n, \omega_n)} = \frac{G_1(0) G_1(2) [\{4G_1(1) + 2G_1(2)\} - k_1 k_3 / k_2^2]}{G_1(1) G_1(3) [6G_1(2) - k_1 k_3 / k_2^2]} \tag{26}$$

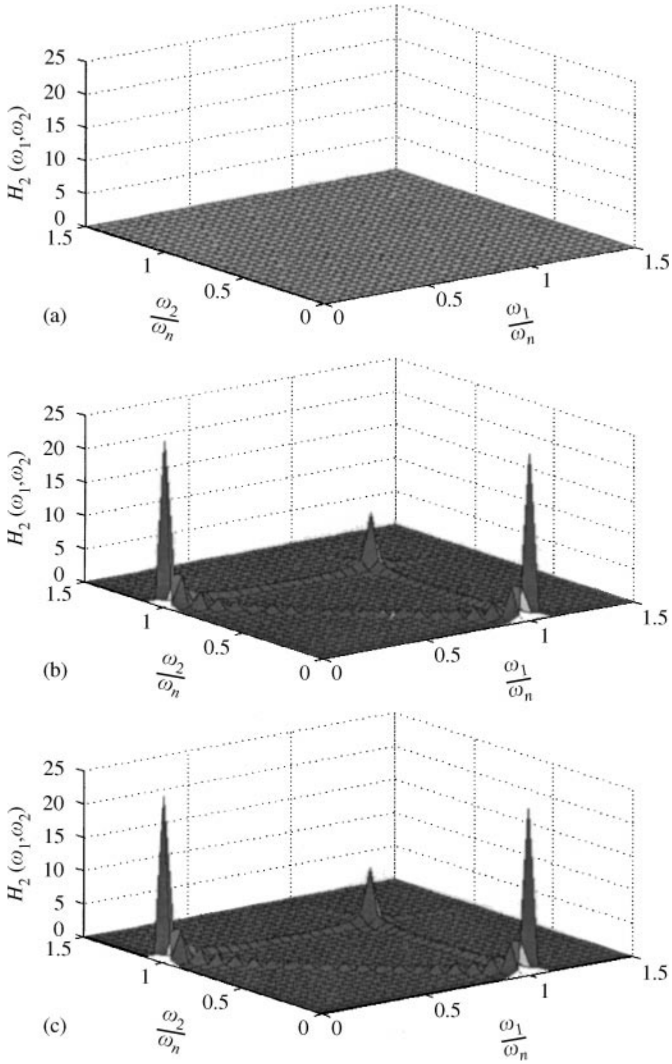

Figure 6. Second-order kernel transform $H_2(\omega_1, \omega_2)$ for various series structures [$\omega_3/\omega_n = 0.6$]: (a) case (i): $k_2 = 0.0$, $k_3 = 0.10$; (b) case (ii): $k_2 = 0.01$, $k_3 = 0.0$; (c) case (iii): $k_2 = 0.01$, $k_3 = 0.0001$.

where $G_1(r)$ is the amplification factor for the frequency ratio $r = \omega/\omega_n$, given as

$$G_1(r) = 1/(1 - r^2 + j2\varsigma r).$$

For $k_3 = 0$, the peak ratio becomes

$$\frac{H_3(0, \omega_n, \omega_n)}{H_3(\omega_n, \omega_n, \omega_n)} = \frac{G_1(0)G_1(2)[\{4G_1(1) + 2G_1(2)\}]}{G_1(1)G_1(3)[6G_1(2)]}. \tag{27}$$

Noting that for small damping, $G_1(1) \gg G_1(2)$, equation (27) can be further simplified as

$$\frac{H_3(0, \omega_n, \omega_n)}{H_3(\omega_n, \omega_n, \omega_n)} = \frac{G_1(0)G_1(2)[4G_1(1)]}{G_1(1)G_1(3)[6G_1(2)]} \approx 5.33. \tag{28}$$

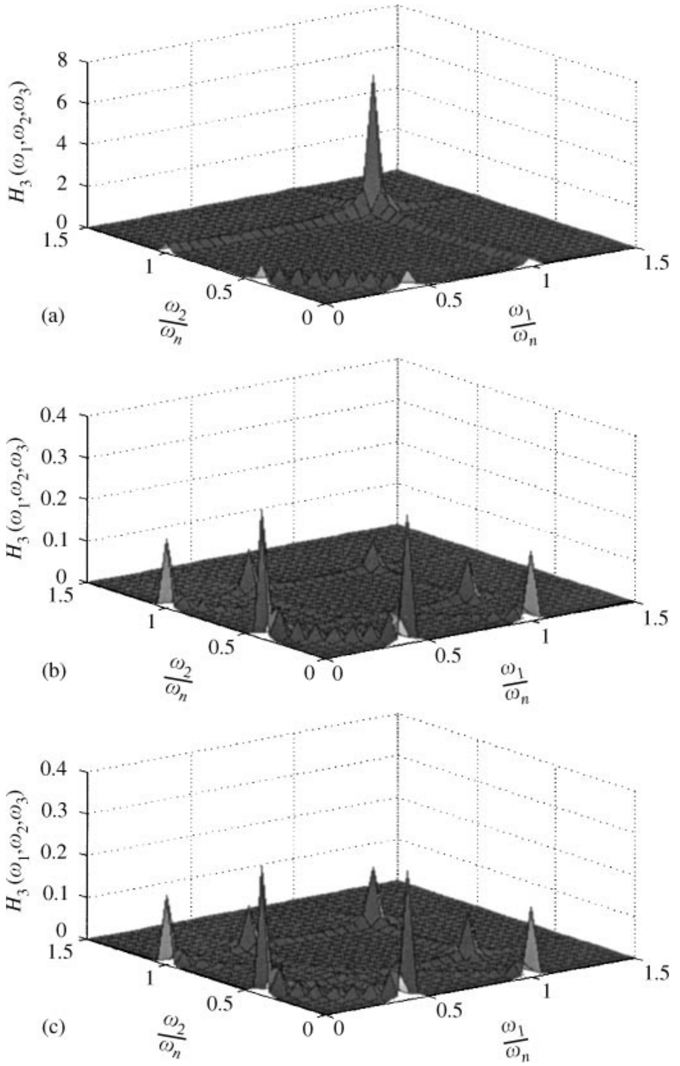

Figure 7. Third-order kernel transform $H_3(\omega_1, \omega_2, \omega_3)$ for various series structures $[\omega_3/\omega_n = 0.6]$: (a) case (i): $k_2 = 0.0$, $k_3 = 0.01$; (b) case (ii): $k_2 = 0.01$, $k_3 = 0.0$; (c) case (iii): $k_2 = 0.01$, $k_3 = 0.0001$.

Similarly for $k_2 = 0$

$$\frac{H_3(0, \omega_n, \omega_n)}{H_3(\omega_n, \omega_n, \omega_n)} = \frac{H_1(0)H_1(2\omega_n)}{H_1(\omega_n)H_1(3\omega_n)} = \frac{G_1(0)G_1(2)}{G_1(1)G_1(3)}. \tag{29}$$

Neglecting damping in the expression of $G_1(2)$ and $G_1(3)$ and noting $G_1(1) = 1/2\varsigma$, the peak ratio becomes

$$\left| \frac{H_3(0, \omega_n, \omega_n)}{H_3(\omega_n, \omega_n, \omega_n)} \right| \approx 5.33\varsigma. \tag{30}$$

It can be concluded, thus, that the peak ratio varies between a maximum value of 5.33 for $k_3 = 0$ to a low value of 5.33ς for $k_2 = 0$. This is highlighted in Fig. 9, where the peak ratio

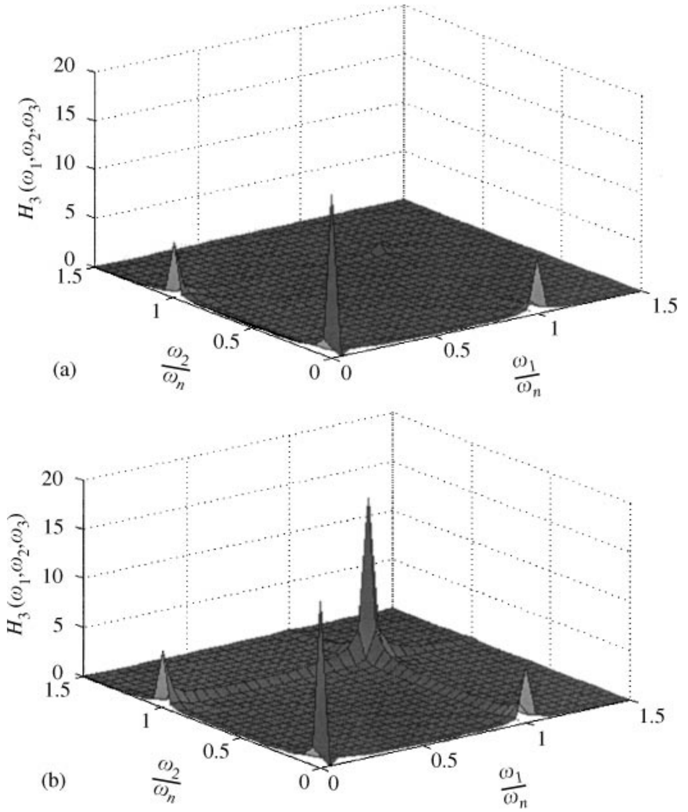

Figure 8. Third-order kernel transform $H_3(\omega_1, \omega_2, \omega_3)$ for cases (ii) and (iii): (a) case (ii): [$k_2 = 0.01$, $k_3 = 0.0$; (b) case (iii): $k_2 = 0.01$, $k_3 = 0.001$.

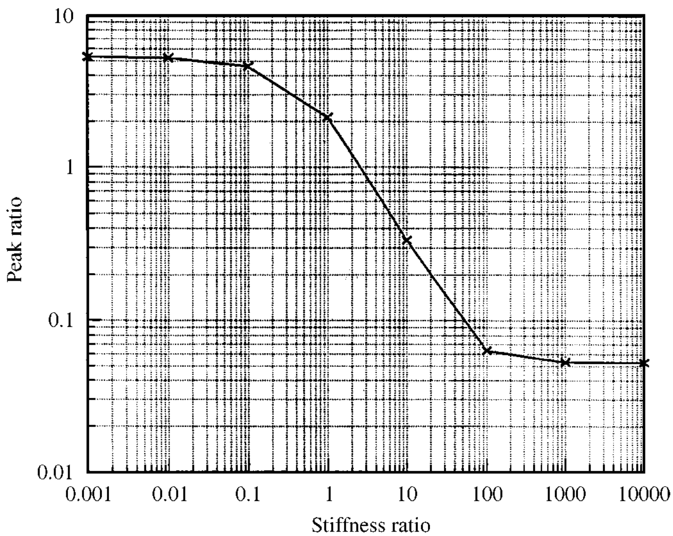

Figure 9. Peak ratio $H_3(0, \omega_n, \omega_n)/H_3(\omega_n, \omega_n, \omega_n)$ *vs* non-dimensional stiffness ratio $\eta = k_1 k_3/k_2^2$.

$H_3(0, \omega_n, \omega_n)/H_3(\omega_n, \omega_n, \omega_n)$ is plotted as a function of non-dimensional stiffness ratio $k_1 k_3/k_2^2$, for a typical damping $\varsigma = 0.01$. The peak ratio, can be seen to be high and nearly constant at 5.0, upto a value of $k_1 k_3/k_2^2$ equal to 0.01 and a system showing such characteristic can be deemed to belong to case (ii), with the cubic term zero. The peak ratio is low and nearly constant at 0.05 for value of $k_1 k_3/k_2^2$ larger than 1000.0. Such a characteristic feature can be employed to categorise the system to case (i). The intermediate values on the graph of Fig. 9 can be taken to characterise systems belonging to case (iii), where both square and cubic powers of $x(t)$ are present in the non-linear restoring force function.

6. REMARKS

Usage of the described higher-order FRF analysis, for non-linearity classification, however need to be guarded against the problem of convergence of the Volterra series [18]. Errors can be expected, particularly in the estimates of non-linear parameters for large response amplitudes. Errors may also arise due to measurement noise, which is not discussed here.

ACKNOWLEDGEMENTS

The authors wish to express their thanks to the financial aid being provided by the Propulsion Panel of Aeronautical Research and Development Board, Ministry of Defence, Government of India, in carrying out this study.

REFERENCES

1. S. R. IBRAHIM 1973 *Shock and Vibration Bulletin* **43**, 21–25. Time domain modal vibration test techniques.
2. D. J. EWINS 1984 *Modal Testing: Theory and Practice*. England: Research Studies Press.
3. R. A. HABER and H. UNBEHAUEN 1990 *Automatica* **26**, 651–677. Structure identification of nonlinear dynamic systems—a survey on input/output approaches.
4. S. BOYD, Y. TANG and L. O. CHUA 1983 *IEEE Transactions on Circuits and Systems* **30**, 571–577. Measuring Volterra kernels.
5. L. O. CHUA and Y. LIAO 1989 *International Journal of Circuit Theory and Applications* **17**, 151–190. Measuring Volterra kernels (II).
6. L. O. CHUA and Y. LIAO 1991 *International Journal of Circuit Theory and Applications* **19**, 189–209. Measuring volterra kernels III: how to estimate the highest significant order.
7. S. F. MASRI, H. SASSI and T. K. CAUGHY 1979 *ASME Transactions Journal of Applied Mechanics* **46**, 433–447. A non-parametric identification technique for nonlinear dynamic problems.
8. S. F. MASRI and T. K. CAUGHY 1982 *ASME Transactions Journal of Applied Mechanics* **49**, 619–627. Non-parametric identification of nearly arbitrary nonlinear systems.
9. H. J. RICE and J. A. FITZPATRICK 1991 *ASME Transactions Journal of Vibration and Acoustics* **113**, 132–140. The measurement of nonlinear damping of single-degree-of-freedom systems.
10. J. E. MOTTERSHED and R. STANWAY 1986 *Journal of Sound and Vibration* **105**, 309–319. Identification of *n*th-power damping.
11. J. S. BENDAT and A G. PIERSOL 1986 *Journal of Sound and Vibration* **106**, 391–408. Decomposition of wave forces into linear and nonlinear components.
12. R. TIWARY and N. S. VYAS 1995 *Journal of Sound and Vibration* **187**, 229–239. Estimation of nonlinear stiffness parameters of rolling element bearings from random response of rotor-bearing systems.
13. A. A. KHAN and N. S. VYAS 1999 *Journal of Sound and Vibration* **221**, 805–821. Nonlinear parameter estimation using Volterra and Weiner theories.
14. A. H. NAYFEH 1985 Parametric identification of nonlinear dynamic systems. *Computers & Structures* **20**, 487–493.

15. J. S. Bendat, P. A. Palo and R. N. Coppolino 1992 *Probabilistic Engineering Mechanics* **7**, 43–61. A general identification technique for nonlinear differential equations of motion.
16. A. B. Gardiner 1968 *Electronic Letters* **4**, 224–226. Determination of the linear output signal of a process containing single-valued nonlinearities.
17. R. J. Simpson and H. M. Powers 1972 *Measurements and Control* **5**, 316–321. Correlation techniques for the identification of nonlinear systems.
18. A. Chatterjee and N. S. Vyas 2000 *Journal of Sound and Vibration* **236**, 339–358. Convergence analysis of Volterra series response of nonlinear systems subjected to harmonic excitation.